Design and Implementation of a MPC-based Rear-Wheel Steering Controller for Sports Cars

Alberto Lucchini, Federica Paganelli Azza, Matteo Corno, Simone Formentin and Sergio M. Savaresi

***Abstract*— Active rear-wheel steering is an effective technology to improve the cornering performance of vehicles, enhancing both handling and stability. In this study, a MPC-based rear-wheel steering controller for sport driving conditions is proposed. High performance is achieved by an accurate choice of the linear time-varying (LTV) predictive model. All the fundamental aspects of lateral dynamics, such as tire force saturation, tire relaxation, aerodynamic downforce and load transfer are taken into account. Simulation results on a multi-body vehicle simulator and the details of the real-time implementation complete the paper.**

I. INTRODUCTION

In four-wheel steering vehicles, open-loop controllers can be exploited to improve handling at low speed and stability at high speed or to achieve a zero sideslip angle during cornering maneuvers [1], [2]. To this aim, a speed-dependent ratio between the front and rear steering angles is imposed, with the front and rear wheels steering in the same direction at high speed and in opposite directions at low speed.

Alternatively to four-wheel steering, rear-wheel steering via feedback control can be used to further enhance performance and safety. For instance, it is possible to modify the damping of the yaw mode [3].

Sliding mode control [4] as well as other robust control techniques [5], [6] have been used in this context, with important results in terms of improvement of the vehicle stability and cornering performance during aggressive maneuvers. These works are united by the use of reference models for the generation of the desired steady-state and transient response of the vehicle.

In the field of lateral dynamics control, Model Predictive Control (MPC) has gained a lot of popularity in recent years, proving itself a successful control strategy. Indeed, the improvement of the overall vehicle behaviour, considering performance and safety at the same time, is possible thanks to the formulation of the control problem as an optimization problem. MPC has been successfully applied to the control of active front-wheel steering [7], torque vectoring [8], [9], [10], and various types of over-actuated architectures, including combined four-wheel steering and torque vectoring [11].

In this paper, a MPC-based controller for active rear-wheel steering is designed, focusing on the maximization of performance in the context of sports cars. For this reason, with respect to the existing literature on lateral dynamics control via MPC, a serious effort is placed in the development of a reliable predictive model when driving at the limits of handling. Following the main line of research of [12], [10], [7], [8], [11], a linear-time varying (LTV) predictive model, obtained from the linearization of a nonlinear model at every MPC iteration, is proposed. This approach allows a sufficiently accurate description of the nonlinear vehicle dynamics, while avoiding a non-convex MPC optimization problem. Indeed, despite nonlinear MPC has been successfully applied in the context of lateral dynamics control [13], the computational burden related to non-convex optimization is still an obstacle for real time-implementation.

The novel contributions of this paper are (i) the proposal of a MPC-based rear-wheel steering controller, specifically designed for sport driving conditions, whereas most of the literature focuses on passenger vehicles (ii) the use of a more accurate predictive model with respect to the literature, including the effects of tire force saturation, tire relaxation, aerodynamic downforce, load transfer, and actuators dynamics, which are relevant in the considered context, and (iii) the real-time implementation of the controller, despite the increased complexity of the underlying vehicle model, thanks to the choices made in the MPC formulation and the use of the state-of-the-art solver for quadratic programming problems *OSQP* [14].

The remainder of this work is as follows. In Section II, the simulation environment is presented. In Section III, a nonlinear vehicle model, which is the basis for the formulation of the LTV predictive model, is described and validated. The proposed rear-wheel steering controller is detailed in Section IV and validated in Section V. The details of the real-time implementation and some concluding remarks are given in Section VI and in Section VII, respectively.

II. SIMULATION ENVIRONMENT

The rear-wheel steering controller proposed in this paper is tested in a simulation environment based on the simulation software *VI-Grade CarRealTime*. In particular, a model of a sports car with the parameters summarized in Table I is considered.

The VI-Grade CarRealTime model is complemented by a custom model of the rear-wheel steering actuators, which is realized in Simulink. In particular, the rear wheels are allowed to steer a maximum of $\delta_r^{max} = 1.95°$ in either direction, with limitations on the maximum steering rate dependent on the current vehicle speed. Additionally, a second-order transfer function with a bandwidth of about 2 Hz introduces realistic lag and attenuation between the target wheel angle requested to the actuator and the actual wheel angle imposed by the actuator.

All the authors are with the Department of Electronics, Information and Bioengineering, Politecnico di Milano, Milan, Italy. Email to name.surname@polimi.it.

The controller is implemented in Simulink, exploiting the interface with both MATLAB code and the open-source C solver OSQP [14] for the solution of the MPC optimization problem.

All the simulation results shown in this work are obtained on a flat road with constant friction coefficient $\mu = 1$, corresponding to dry asphalt conditions.

III. NONLINEAR VEHICLE MODEL

The first step in the design of a MPC-based controller is the formulation of a suitable model of the system. Since the vehicle lateral dynamics is characterized by highly nonlinear phenomena, especially because of the road-tire interaction, a nonlinear vehicle model is proposed in the following. The model describes the lateral dynamics only; indeed, the vehicle's longitudinal velocity v_x is treated as a time-varying parameter rather than as a state. Similarly, the longitudinal load transfer is taken into account by considering the vertical forces acting on the wheels as time-varying parameters. Starting from this nonlinear model, in Section IV, a linear time-varying (LTV) predictive model is obtained by linearization.

As schematically represented in Fig. 1, a single-track vehicle model [15] is used, which is a standard solution in the formulation of rear-wheel steering controllers [4], [5], [6]. Under the assumption of small front and rear steering angles (δ_f and δ_r, respectively) and attitude angle β, the following equations of motion can be derived

$$\begin{cases} \dot{r} = \frac{1}{J_z}\left(aF_{yf} - bF_{yr}\right) \\ \dot{\beta} = \frac{1}{Mv_x}\left(F_{yf} + F_{yr}\right) - r, \end{cases} \tag{1}$$

where r is the yaw rate and F_{yf} and F_{yr} are the front and rear axle lateral forces, respectively. M, J_z, a and b are constant parameters representing the mass, yaw moment of inertia and front and rear axle distances from the center of gravity, respectively.

TABLE I: Vehicle parameters.

Definition	Parameter	Value
Mass	M	1930 kg
Yaw inertia	J_z	3554 kg m^2
Wheelbase	L	2720 mm
Front axle distance to COG	a	1461 mm
Rear axle distance to COG	b	1259 mm
Front axle track	d_f	1668 mm
Rear axle track	d_r	1636 mm
Wheel radius	R_w	350 mm

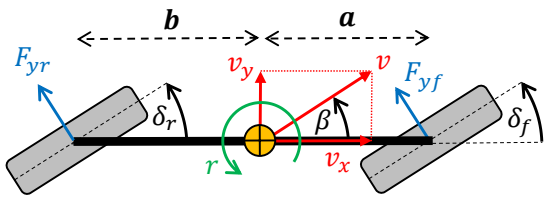

Fig. 1: Single-track vehicle model.

An important element of novelty is introduced in the model of the sideslip angles, which are the fundamental quantities that determine the lateral tire forces. In the literature related to MPC-based lateral dynamics control [12], [7], the lateral tire forces are expressed as an algebraic function of the kinematic sideslip angles α_f^{kin} and α_r^{kin}, which can be computed on the basis of simple geometrical considerations [12]:

$$\alpha_f^{kin} = -\delta_f + \beta + \frac{a}{v_x} r, \quad \alpha_r^{kin} = -\delta_r + \beta - \frac{b}{v_x} r. \tag{2}$$

However, this approach does not consider the relaxation dynamics of the tires [15], which has important effects on the vehicle lateral dynamics. To overcome this issue, a first-order dynamics between the kinematic sideslip angles and the actual sideslip angles (α_f and α_r) is introduced [16], [17]:

$$\dot{\alpha}_j = -\frac{1}{h_j(v_x)}\left(\alpha_j - \alpha_j^{kin}\right), \quad j = f, r, \tag{3}$$

where $h_f(v_x)$ and $h_r(v_x)$ determine the time constant of the relaxation dynamics depending on the vehicle's longitudinal velocity. A possible parametrization of such functions is given by

$$h_j(v_x) = \frac{\bar{h}_j}{v_x}, \quad j = f, r, \tag{4}$$

where the parameters $\bar{h}_f$ and $\bar{h}_r$ can be physically interpreted as tire relaxation lengths [16].

Indicating by F_{zf} and F_{zr} the vertical loads acting on the two axles, the lateral tire forces are modelled by means of a simplified version of Pacejka's Magic Formula [15]:

$$F_{yj} = -f_j(F_{zj}) \frac{C_j}{B_j A_j} \sin(B_j \arctan(A_j \alpha_j)), \quad j = f, r. \tag{5}$$

In (5), the dependence of the lateral tire force on the sideslip angle is determined by the parameters A_j, B_j and C_j, $i = f, r$. Moreover, the tire characteristic curve is rescaled by a factor dependent on the vertical load acting on the axle, namely $f_f\left(F_{zf}\right)$ and $f_r\left(F_{zr}\right)$. This nonlinear relationship can be modelled with a saturation function:

$$\begin{cases} f_j(F_{zj}) = F_{zj}, & F_{zj} < \bar{F}_{zj} \\ f_j(F_{zj}) = \bar{F}_{zj}, & F_{zj} \geq \bar{F}_{zj} \end{cases} \quad j = f, r, \tag{6}$$

where $\bar{F}_{zf}$ and $\bar{F}_{zr}$ are thresholds above which an increase of vertical load does not cause an increase of lateral tire force. Conversely, below those thresholds, the lateral forces are rescaled linearly with respect to the vertical load to describe the effects of longitudinal load transfer and aerodynamic downforce.

The nonlinear vehicle model is completed by the expression of the front wheels steering angle as a function of the steering rack position x_r and vehicle's lateral acceleration $a_y = v_x\left(r + \dot{\beta}\right)$:

$$\delta_f = k_{xr} x_r + k_{ay} a_y \tag{7}$$

where k_{xr} represents the nominal kinematic ratio between the front wheels steering angle and the steering rack position,

while the second term models the variation of steering angle due to the suspension kinematics during maneuvers with significant lateral acceleration.

The resulting vehicle model is the following fourth-order nonlinear model

$$\begin{cases} \dot{r} = \frac{1}{J_z}\left(aF_{yf}\left(\alpha_f, F_{zf}\right) - bF_{yr}\left(\alpha_r, F_{zr}\right)\right) \\ \dot{\beta} = \frac{1}{Mv_x}\left(F_{yf}\left(\alpha_f, F_{zf}\right) + F_{yr}\left(\alpha_r, F_{zr}\right)\right) - r \\ \dot{\alpha}_f = -\frac{1}{h_f(v_x)}\left(\alpha_f + k_{xr}x_r + k_{ay}v_x\left(r + \dot{\beta}\right) - \beta - \frac{a}{v_x}r\right) \\ \dot{\alpha}_r = -\frac{1}{h_r(v_x)}\left(\alpha_r + \delta_r - \beta + \frac{b}{v_x}r\right), \end{cases} \tag{8}$$

where r, β, α_f and α_r are the state variables, x_r and δ_r are the inputs, F_{zf}, F_{zr} and v_x are time-varying parameters. All the other parameters are selected to fit the VI-Grade CarRealTime model. In particular, the parameters reported in Table I are assumed to be known, while the remaining ones are identified via simulation experiments.

Validation tests are performed by feeding the model with the steering rack position x_r and the rear steering angle δ_r collected during appropriate VI-Grade CarRealTime simulations and assuming exact knowledge of the time-varying parameters, namely the longitudinal velocity v_x and the vertical forces acting on the two axles F_{zf} and F_{zr}. For comparison, the results obtained with a simplified second-order model, similar to the one tipically used in the literature, are also reported. Such a model is obtained from (8) by neglecting both the tire relaxation dynamics (by setting $\alpha_f = \alpha_f^{kin}$ and $\alpha_r = \alpha_r^{kin}$) and the effects of load transfer and aerodynamic downforce (by setting the vertical forces F_{zf} and F_{zr} equal to their steady-state value at $100\,\mathrm{km\,h^{-1}}$). In the following, this latter model will be indicated as "simplified", while the proposed vehicle model as "complete".

The validation test shown in Fig. 2 consists in a frequency sweep of the steering wheel angle from 0.5 Hz to 3.5 Hz at a constant speed of $100\,\mathrm{km\,h^{-1}}$. Even if the test is very dynamic and reaches high lateral accelerations, the simulation of the complete vehicle model yields very accurate results. Conversely, the simplified model shows a remarkably decreased ability to fit the VI-Grade CarRealTime simulation, due to the neglection of the tire relaxation dynamics.

In Fig. 3, a slow ramp steer maneuver while braking from $250\,\mathrm{km\,h^{-1}}$ to $100\,\mathrm{km\,h^{-1}}$ is shown. Once again, the complete vehicle model is capable to reproduce the VI-Grade CarRealTime simulation very closely. On the contrary, the performance of the simplified model is significantly inferior, since it does not account for the longitudinal load transfer and the variation of the aerodynamic downforce.

IV. MODEL PREDICTIVE CONTROLLER DESIGN

The main purpose of this section is to describe the MPC optimization problem, which is the core of the proposed rear-wheel steering controller. To this aim, all the steps for the initialization of the optimization problem, the computation of the (linerized) predictive model and the generation of a suitable yaw rate reference are described first.

Vehicle state estimation. As detailed in the following, the MPC predictive model is obtained from the linearization of the nonlinear vehicle model described in Section III. As a consequence, the setup of the MPC optimization problem requires the computation of appropriate initialization values for the four states of the vehicle model.

Concerning the vehicle's yaw rate and attitude angle, the initialization values r_0^i and β_0^i at the i-th MPC iteration are set to

$$r_0^i = \hat{r}(t_i), \quad \beta_0^i = \hat{\beta}(t_i), \tag{9}$$

where $\hat{r}(t_i)$ and $\hat{\beta}(t_i)$ are the current yaw rate and attitude angle measurements provided by two ideal sensors and t_i is the time instant corresponding to the i-th MPC iteration. Notice that the attitude angle would be estimated in a real-world application.

Conversely, the initialization of the sideslip angles cannot be directly obtained from measurements or estimations. Thus, their value is computed online, compatibly with the control-oriented tire relaxation model proposed above. Combining (2), (3) and (7), it results that

$$\begin{cases} \dot{\alpha}_f = -\frac{1}{h_f(v_x)}\left(\alpha_f + k_{xr}x_r + k_{ay}a_y - \beta - \frac{a}{v_x}r\right) \\ \dot{\alpha}_r = -\frac{1}{h_r(v_x)}\left(\alpha_r + \delta_r - \beta + \frac{b}{v_x}r\right). \end{cases} \tag{10}$$

Then, assuming that measurements of the current vehicle's longitudinal velocity, lateral acceleration, steering rack position and rear wheels steering angle are available (indicated by $\hat{v}_x(t_i)$, $\hat{a}_y(t_i)$, $\hat{x}_r(t_i)$ and $\hat{\delta}_r(t_i)$, respectively), the initialization value of the sideslip angles can be computed from a discrete time version of (10), that is

$$\begin{cases} \alpha_{f0}^i = u_f\left(\alpha_{f0}^{i-1}, \hat{r}(t_i), \hat{\beta}(t_i), \hat{x}_r(t_i), \hat{a}_y(t_i), \hat{v}_x(t_i)\right) \\ \alpha_{r0}^i = u_r\left(\alpha_{r0}^{i-1}, \hat{r}(t_i), \hat{\beta}(t_i), \hat{\delta}_r(t_i), \hat{v}_x(t_i)\right). \end{cases} \tag{11}$$

Non-controllable inputs and time-varying model parameters. In order to predict the evolution of the controlled system over the prediction horizon, the MPC-based controller requires to know the future values of all the non-controllable inputs and time-varying parameters appearing in the predictive model. Since this is not possible in practice, an approximation of those signals is computed based on the available information up to the current time.

In the case at hand, the only non-controllable input is the steering rack position, whose value is imposed by the driver acting on the steering wheel. A first-order extrapolation of the signal is computed based on the current steering rack speed $\hat{\dot{x}}_r(t_i)$, which is assumed to remain approximately constant for the duration of the prediction horizon:

$$x_r^i(k) = \hat{x}_r(t_i) + (kT_p)\,\hat{\dot{x}}_r(t_i), \quad k = 0, \ldots, N_p - 1, \tag{12}$$

where the index k refers to the k-th step along the prediction horizon, N_p is the number of steps in the prediction horizon, and T_p is the time step.

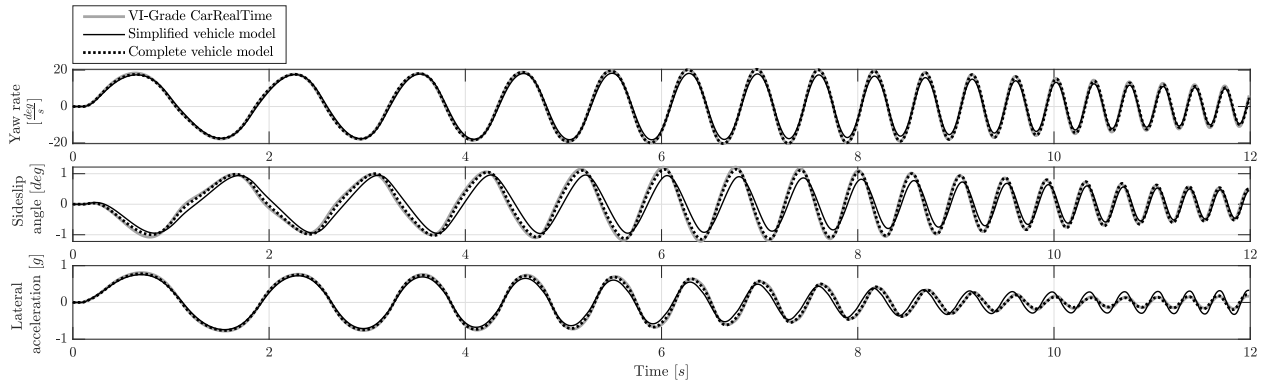

Fig. 2: Validation of the vehicle model: frequency sweep of steering wheel angle from 0.5 Hz to 3.5 Hz at 100 km h^{-1}.

Regarding the time-varying model parameters, the assumption of constancy over the prediction horizon is made. In particular, at every iteration of the control algorithm, the longitudinal velocity of the vehicle is set to the measured value at the current time t_i, that is $\bar{v}_x^i = \hat{v}_x(t_i)$.

Similarly, the vertical forces acting on each axle are fixed to the estimated value at time t_i, indicated by $\hat{F}_{zf}(t_i)$ and $\hat{F}_{zr}(t_i)$ for the front and rear axles, respectively:

$$\bar{F}_{zf}^i = \hat{F}_{zf}(t_i), \quad \bar{F}_{zr}^i = \hat{F}_{zr}(t_i). \tag{13}$$

In order to compute such values, the following model of the vehicle's longitudinal load transfer and aerodynamics is used:

$$\begin{cases} \hat{F}_{zf}(t_i) = \frac{b}{L} Mg - k_{ax}\hat{a}_x(t_i) + k_{vxf}\hat{v}_x(t_i)^2 \\ \hat{F}_{zr}(t_i) = \frac{a}{L} Mg + k_{ax}\hat{a}_x(t_i) + k_{vxr}\hat{v}_x(t_i)^2, \end{cases} \tag{14}$$

where $\hat{a}_x(t_i)$ is the measured longitudinal acceleration and g is the gravitational acceleration. According to the model in (14), the longitudinal load transfer is proportional to the longitudinal acceleration through the parameter k_{ax}, while the aerodynamic downforce on the two axles is proportional to the square of the vehicle speed through the parameters k_{vxf} and k_{vxr}.

Vehicle model linearization. The use of a nonlinear predictive model results in a non-convex MPC optimization problem, to be solved at every time step. This solution, although possible [13], implies a relevant computational burden, which may prevent the real-time implementation of the controller. To overcome this issue, the approach based on successive online linearizations of the model around the current operating point is usually preferred [7], [12]. In this way, the nonlinear vehicle dynamics can be accounted for, while significantly reducing the complexity of the optimization problem.

To linearize the vehicle model, it is sufficient to linearize the expressions in (5) around the current sideslip angles α_{f0}^i and α_{r0}^i, after substituting the current vertical loads $\bar{F}_{zf}^i$ and $\bar{F}_{zr}^i$:

$$F_{yf} = \bar{F}_{yf}^i - \bar{C}_f^i\left(\alpha_f - \alpha_{f0}^i\right), \quad F_{yr} = \bar{F}_{yr}^i - \bar{C}_r^i\left(\alpha_r - \alpha_{r0}^i\right). \tag{15}$$

The resulting predictive model at the i-th MPC iteration is the following fourth-order affine system:

$$\dot{x} = A^i x + B^i \delta_r + C^i x_r + D^i, \quad x = \begin{bmatrix} r & \beta & \alpha_f & \alpha_r \end{bmatrix}^T, \tag{16}$$

where

$$A^i = \begin{bmatrix} 0 & 0 & -\frac{a\bar{C}_f^i}{J_z} & \frac{b\bar{C}_r^i}{J_z} \\ -1 & 0 & -\frac{\bar{C}_f^i}{M\bar{v}_x^i} & -\frac{\bar{C}_r^i}{M\bar{v}_x^i} \\ \frac{a}{h_f(\bar{v}_x^i)\bar{v}_x^i} & \frac{1}{h_f(\bar{v}_x^i)} & \frac{k_{ay}\bar{C}_f^i - M}{Mh_f(\bar{v}_x^i)} & \frac{k_{ay}\bar{C}_r^i}{Mh_f(\bar{v}_x^i)} \\ -\frac{b}{\bar{v}_x^i h_r(\bar{v}_x^i)} & \frac{1}{h_r(\bar{v}_x^i)} & 0 & -\frac{1}{h_r(\bar{v}_x^i)} \end{bmatrix}, \tag{17a}$$

$$B^i = \begin{bmatrix} 0 & 0 & 0 & \frac{1}{h_r(\bar{v}_x^i)} \end{bmatrix}^T, \tag{17b}$$

$$C^i = \begin{bmatrix} 0 & 0 & -\frac{k_{xr}}{h_f(\bar{v}_x^i)} & 0 \end{bmatrix}^T, \tag{17c}$$

$$D^i = \begin{bmatrix} \frac{a\left(\bar{F}_{yf}^i + \bar{C}_f^i\alpha_{f0}^i\right) - b\left(\bar{F}_{yr}^i + \bar{C}_r^i\alpha_{r0}^i\right)}{J_z} \\ \frac{\bar{F}_{yf}^i + \bar{C}_f^i\alpha_{f0}^i + \bar{F}_{yr}^i + \bar{C}_r^i\alpha_{r0}^i}{M\bar{v}_x^i} \\ -\frac{k_{ay}\left(\bar{F}_{yf}^i + \bar{C}_f^i\alpha_{f0}^i + \bar{F}_{yr}^i + \bar{C}_r^i\alpha_{r0}^i\right)}{Mh_f(\bar{v}_x^i)} \\ 0 \end{bmatrix}. \tag{17d}$$

Rear-wheel steering actuator model. The predictive model computed above is further extended to take into account the dynamics of the rear-wheel steering actuators. A first-order dynamics between the reference steering angle δ_r^{ref} and the actual steering angle δ_r is introduced as follows

$$\begin{cases} \dot{x} = A^i x + B^i \delta_r + C^i x_r + D^i \\ \dot{\delta}_r = -\omega_{act}\left(\delta_r - \delta_r^{ref}\right). \end{cases} \tag{18}$$

Notice that a low-order actuator model is used to avoid an excessive increase of the dimension of the predictive model. Concerning the initialization of the newly introduced state, the current measured value is used, that is $\delta_{r0}^i = \hat{\delta}_r(t_i)$.

Yaw rate reference generation. A yaw rate signal describing the desired behaviour of the vehicle over the prediction horizon is used as a reference for the MPC. The yaw rate reference is computed as a function of the steering wheel angle δ_{sw} imposed by the driver and the vehicle speed v_x, using a static map of the form

$$r_{des} = r_{des}(\delta_{sw}, v_x). \tag{19}$$

In this way, it is possible to impose a desired understeering behaviour to the controlled vehicle [8].

In particular, a sequence of samples $\{\delta^i_{sw}(k)\}_{k=1}^{N_p}$ representing the expected steering wheel angle over the prediction horizon is computed by linear extrapolation (as in (12)) and, given the current vehicle speed $\bar{v}^i_x$, the corresponding yaw rate sequence $\{r^i_{des}(k)\}_{k=1}^{N_p}$ is obtained. Lastly, a low-pass filter is applied to this sequence, obtaining the actual reference signal $\{r^i_{ref}(k)\}_{k=1}^{N_p}$. A certain number of yaw rate reference samples from the previous MPC iterations ($r^{i-1}_{ref}(1)$, $r^{i-2}_{ref}(1)$, etc.) are used for the initialization of the filter, depending on its dynamical order. The filter is chosen so as to reduce the yaw rate resonance of the vehicle and to avoid possibly dangerous behaviour of the controlled vehicle in response to high-frequency steering inputs.

MPC optimization problem. At every MPC iteration, the optimal control sequence $\{\delta^{ref}_r(k)\}_{k=0}^{N_p-1}$ over the prediction horizon is computed by solving the following optimization problem, which can be rewritten as a quadratic programming (QP) problem:

$$\min_{\delta^{ref}_r(\cdot)} \quad \sum_{k=1}^{N_p} \left(r(k) - r^i_{ref}(k)\right)^2 \tag{20a}$$

$$\text{s.t.} \quad \xi(k+1) = A_d\xi(k) + B_d\delta^{ref}_r(k) + C_d x_r(k) + D_d \quad k = 1, \ldots, N_p \tag{20b}$$

$$\xi(0) = \begin{bmatrix} r^i_0 & \beta^i_0 & \alpha^i_{f0} & \alpha^i_{r0} & \delta^i_{r0} \end{bmatrix}^T \tag{20c}$$

$$|\delta_r(k)| \leq \delta^{max}_r \quad k = 0, \ldots, N_p - 1 \tag{20d}$$

$$|\delta_r(k) - \delta_r(k-1)| \leq \Delta\delta_r(\bar{v}^i_x) \quad k = 0, \ldots, N_p - 1, \tag{20e}$$

where the matrices A_d, B_d, C_d, D_d are obtained from the time discretization of (18) using Euler's method and $\xi = \begin{bmatrix} r & \beta & \alpha_f & \alpha_r & \delta_r \end{bmatrix}^T$ is the corresponding state vector.

Notice that the cost function (20a) includes a single objective for the controlled vehicle, that is to track the yaw rate reference over the prediction horizon.

The constraints (20b) and (20c) impose the dynamics of the controlled vehicle, relating the sequence of the control inputs to the predicted evolution of the controlled system, starting from the currently estimated state.

Lastly, the constraints (20d) and (20e) account for the limitations of the rear-wheel steering actuators in terms of both maximum steering angle and maximum steering rate, *i.e.* the ones described in Section II.

Once the MPC optimization problem is solved, according to the standard receiding horizon approach, only the first sample $\delta^{ref}_f(0)$ of the optimal control sequence is applied to the system. Then, an updated optimization problem is solved again at the next MPC iteration.

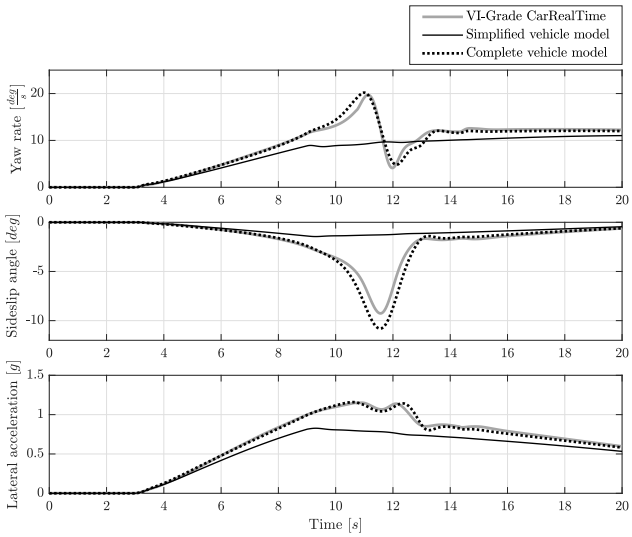

Fig. 3: Validation of the vehicle model: slow ramp steer maneuver while braking from $250\,\mathrm{km\,h^{-1}}$ to $100\,\mathrm{km\,h^{-1}}$.

Concerning the choice of the MPC parameters, such as the length of the prediction horizon N_p and the time step T_p, it is observed that a reasonable comprimise between computational load and performance is achieved by setting $T_p = 0.01\,\mathrm{s}$ and $N_p = 15$, which is in line with the results of other MPC-based lateral dynamics controllers in the literature [7], [8].

V. ANALYSIS AND VALIDATION

Simulations are performed to evaluate the performance of the proposed rear-wheel steering controller. In particular, a number of different handling maneuvers, including combined cornering and traction/braking, are analyzed. A few simulation results are reported in the following.

In Fig. 4 a step-steer maneuver at the constant speed of $150\,\mathrm{km\,h^{-1}}$ is shown. It is possible to see that the MPC-based controller is able to track the yaw rate reference (computed by collecting the first samples of the reference signals of every MPC iteration) very closely. Moreover, notice that the ratio between the peak and the steady-state value of the yaw rate is significantly reduced with respect to the uncontrolled vehicle.

In Fig. 5 a slow ramp steer maneuver while braking from $250\,\mathrm{km\,h^{-1}}$ to $100\,\mathrm{km\,h^{-1}}$ is reported. Once again, the MPC controlled vehicle follows the yaw rate reference very well. While the uncontrolled vehicle is driven very close to instability, the MPC controlled vehicle shows a very limited attitude angle and no oscillations of the yaw rate.

VI. REAL-TIME IMPLEMENTATION

As already pointed out, the MPC optimization problem in (20) can be easily rewritten as a QP problem, for which very efficient open-source solvers are available. Among them,

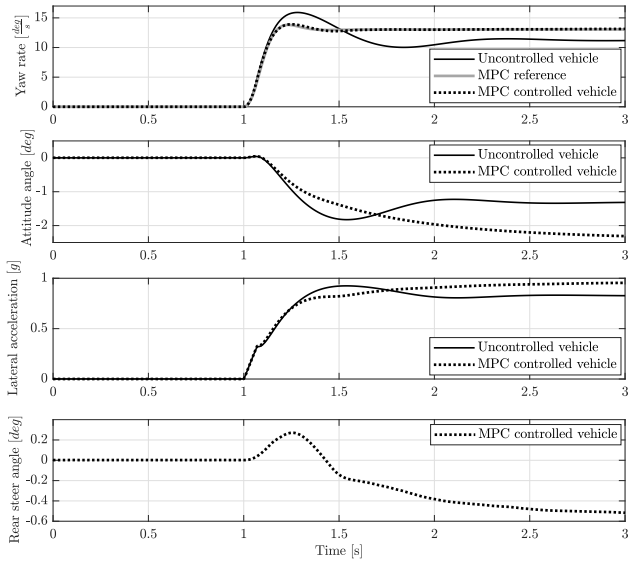

Fig. 4: MPC performance in a step-steer maneuver at $150\,\mathrm{km\,h^{-1}}$.

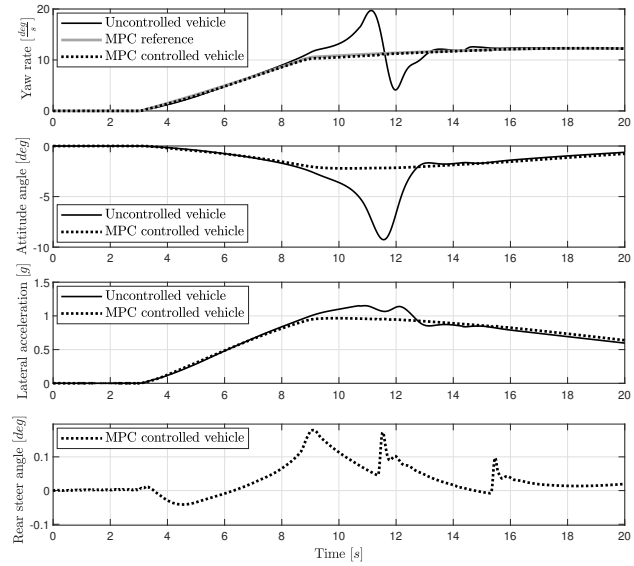

Fig. 5: MPC performance in a slow ramp steer maneuver while braking from $250\,\mathrm{km\,h^{-1}}$ to $100\,\mathrm{km\,h^{-1}}$.

OSQP is particularly well-suited for use on embedded low-power hardware [14], [18], as it allows to generate fast and reliable C code for this kind of problems.

This option is exploited in this work to implement the proposed control algorithm on the *dSpace MicroAutobox II* hardware and assess the feasibility of a real-time implementation. On the considered hardware, the average computational time required by the controller is about 1.5 ms, which is satisfactory since the controller time step is $T_p = 0.01\,\mathrm{s}$.

VII. CONCLUSIONS

A MPC-based rear-wheel steering controller is presented in this paper and validated in a realistic simulation environment. Thanks to the modelling choices, excellent performance is achieved in the tracking of a yaw rate reference, even in very dynamic maneuvers. The feasibility of a real time implementation on low-power hardware is also demonstrated.

Based on these promising results, future work will be devoted to the experimental validation of the controller on a real-world setup.

REFERENCES

[1] S. Sano, Y. Furukawa, and S. Shiraishi, "Four wheel steering system with rear wheel steer angle controlled as a function of steering wheel angle," *SAE Transactions*, pp. 880–893, 1986.

[2] Y. Furukawa, N. Yuhara, S. Sano, H. Takeda, and Y. Matsushita, "A review of four-wheel steering studies from the viewpoint of vehicle dynamics and control," *Vehicle system dynamics*, vol. 18, no. 1-3, pp. 151–186, 1989.

[3] J. Ackermann and W. Sienel, "Robust yaw damping of cars with front and rear wheel steering," *IEEE Transactions on Control Systems Technology*, vol. 1, no. 1, pp. 15–20, 1993.

[4] T. Hiraoka, O. Nishihara, and H. Kumamoto, "Model-following sliding mode control for active four-wheel steering vehicle," *Review of Automotive Engineering*, vol. 25, no. 3, p. 305, 2004.

[5] M. Ariff, H. Zamzuri, M. Nordin, W. Yahya, S. Mazlan, and M. Rahman, "Optimal control strategy for low speed and high speed four-wheel-active steering vehicle," *Journal of Mechanical Engineering and Sciences*, vol. 8, pp. 1516–1528, 2015.

[6] H. Lv and S. Liu, "Closed-loop handling stability of 4ws vehicle with yaw rate control," *Strojniški vestnik-Journal of Mechanical Engineering*, vol. 59, no. 10, pp. 595–603, 2013.

[7] C. E. Beal and J. C. Gerdes, "Model predictive control for vehicle stabilization at the limits of handling," *IEEE Transactions on Control Systems Technology*, vol. 21, no. 4, pp. 1258–1269, 2012.

[8] A. Lucchini, S. Formentin, M. Corno, D. Piga, and S. M. Savaresi, "Torque vectoring for high-performance electric vehicles: An efficient mpc calibration," *IEEE Control Systems Letters*, vol. 4, no. 3, pp. 725–730, 2020.

[9] M. Jalali, A. Khajepour, S.-k. Chen, and B. Litkouhi, "Integrated stability and traction control for electric vehicles using model predictive control," *Control Engineering Practice*, vol. 54, pp. 256–266, 2016.

[10] O. Barbarisi, G. Palmieri, S. Scala, and L. Glielmo, "Ltv-mpc for yaw rate control and side slip control with dynamically constrained differential braking," in *2009 European Control Conference (ECC)*. IEEE, 2009, pp. 4810–4815.

[11] M. Ataei, A. Khajepour, and S. Jeon, "Model predictive control for integrated lateral stability, traction/braking control, and rollover prevention of electric vehicles," *Vehicle system dynamics*, vol. 58, no. 1, pp. 49–73, 2020.

[12] P. Falcone, F. Borrelli, J. Asgari, H. E. Tseng, and D. Hrovat, "A model predictive control approach for combined braking and steering in autonomous vehicles," in *2007 Mediterranean Conference on Control & Automation*. IEEE, 2007, pp. 1–6.

[13] F. Borrelli, P. Falcone, T. Keviczky, J. Asgari, and D. Hrovat, "Mpc-based approach to active steering for autonomous vehicle systems," *International journal of vehicle autonomous systems*, vol. 3, no. 2-4, pp. 265–291, 2005.

[14] B. Stellato, G. Banjac, P. Goulart, A. Bemporad, and S. Boyd, "OSQP: an operator splitting solver for quadratic programs," *Mathematical Programming Computation*, vol. 12, no. 4, pp. 637–672, 2020. [Online]. Available: https://doi.org/10.1007/s12532-020-00179-2

[15] H. Pacejka, *Tire and vehicle dynamics*. Elsevier, 2005.

[16] J. S. Loeb, D. A. Guenther, H.-H. F. Chen, and J. R. Ellis, "Lateral stiffness, cornering stiffness and relaxation length of the pneumatic tire," *SAE transactions*, pp. 147–155, 1990.

[17] G. J. Heydinger, W. R. Garrott, and J. P. Chrstos, "The importance of tire lag on simulated transient vehicle response," *SAE transactions*, pp. 362–374, 1991.

[18] G. Banjac, B. Stellato, N. Moehle, P. Goulart, A. Bemporad, and S. Boyd, "Embedded code generation using the OSQP solver," in *IEEE Conference on Decision and Control (CDC)*, 2017. [Online]. Available: https://doi.org/10.1109/CDC.2017.8263928